Physics – Uspekhi **62** (11) 1126 – 1135 (2019) ©2019 Uspekhi Fizicheskikh Nauk, Russian Academy of Sciences

CONFERENCES AND SYMPOSIA

PACS numbers: 07.05.Tp, **97.30. – b,** 97.80.Jp

Accretion processes in astrophysics

N I Shakura, D A Kolesnikov, K A Postnov, I M Volkov, I F Bikmaev, T R Irsmambetova, R Staubert, J Wilms, E Irtuganov, P Shurygin, P Yu Golysheva, S Yu Shugarov, I V Nikolenko, E M Trunkovsky, G Schoenherr, A Schwope, D Klochkov

DOI: https://doi.org/10.3367/UFNe.2019.04.038647

Contents

Abstract. Accretion onto magnetized neutron stars is considered using as a case study long-term X-ray and optical observations of HZ Her/Her X-1, an X-ray binary system with a 1.7-day orbital period where disc accretion occurs from the optical donor star (HZ Her) onto a neutron star (Her X-1). On top of orbital variability and pulsating X-ray emission from the neutron star rotating with a period of about one second, a 35-day X-ray modulation of emission is observed. The 35-day variability is due to a tilted precessing accretion disc that periodically screens X-ray emission from the neutron star. The disc precession that occurs in the direction opposite to the orbital motion is determined by the joint action of the tidal torque from the donor and dynamical torque from the gas streams. Several dozen thousand broadband UBV photometric observations of HZ Her have been obtained since 1972. The shape of the orbital light curves of HZ Her also changes with the 35-day cycle phase. The orbital variability can be reproduced in a model that includes a precessing tilted and warped accretion disc around a freely precessing neutron star. The disc is warped near its inner edge due to interaction with the rotating neutron star magnetosphere. The magnetic torque depends on the precessional phase of the neutron star. The X-ray emission flux from the neutron star also depends on the free precession phase that modulates the heating of the optical-star atmosphere and the intensity of gas streams. We show that this model reproduces well both optical observations of HZ Her and the behavior of the 35-day X-ray cycle.

Keywords: accretion discs, X-ray binaries, neutron stars, modeling

N I Shakura [1, 2, a], **D A Kolesnikov** [1, b], **K A Postnov** [1, 2, c], **I M Volkov** [1, 3], **I F Bikmaev** [2, d], **T R Irsmambetova** [1], **R Staubert** [4], **J Wilms** [5], **E Irtuganov** [2], **P Shurygin** [2], **P Yu Golysheva** [1], **S Yu Shugarov** [1, 6], **I V Nikolenko** [3, 7], **E M Trunkovsky** [1], **G Schoenherr** [8], **A Schwope** [8], **D Klochkov** [4]

[1] Lomonosov Moscow State University,
Sternberg State Astronomical Institute,
Universitetskii prosp. 13, 119234 Moscow, Russian Federation
[2] Kazan Federal University,
ul. Kremlevskaya 18, 420008 Kazan, Russian Federation
[3] Institute of Astronomy, Russian Academy of Sciences,
ul. Pyatnitskaya 48, 119017 Moscow, Russian Federation
[4] Institute for Astronomy and Astrophysics,
Geschwister-Scholl-Platz, 72074 Tübingen, Germany
[5] Astronomical Institute of the University of Erlangen-Nuremberg,
Sternwart str. 7, 96049 Bamberg, Germany
[6] Astronomical Institute, Slovak Academy of Sciences,
Tatranska Lomnica, SK 059 60 Slovakia
[7] Crimean Astrophysical Observatory, Russian Academy of Sciences,
pos. Nauchny, 298409 Bakhchisarai district, Republic of Crimea,
Russian Federation
[8] Leibniz Institute for Astrophysics Potsdam,
An der Sternwarte 16, 14482 Potsdam, Germany
E-mail: [a] nikolai.shakura@gmail.com, [b] kolesnikovkda@gmail.com,
[c] kpostnov@gmail.com, [d] ibikmaev@yandex.ru

Received 26 July 2019
Uspekhi Fizicheskikh Nauk **189** (11) 1202 – 1212 (2019)
DOI: https://doi.org/10.3367/UFNr.2019.04.038647
Translated by K A Postnov; edited by V L Derbov

1. Introduction. Origin of accretion

At the beginning of the 1970s, a major discovery in modern natural science occurred — the first X-ray satellite in human history, Uhuru, discovered accreting black holes and neutron stars in stellar binary systems [1, 2]. This discovery provided a huge impetus in the development of a new topic in high-energy astrophysics: research of accretion processes around black holes, neutron stars, and other gravitating bodies. The discovery had been anticipated. Ten years earlier, a space rocket equipped with X-ray detectors discovered the first X-ray source far outside the Solar System [3]. The source was

named Sco X-1 by its location in the direction toward the Scorpius constellation. The discovery of Sco X-1 was accidental, because the true goal of the experiment was to discover the fluorescent X-ray glow from the Moon's surface. Subsequent rocket launches discovered new X-ray sources, including Cyg X-1, Cyg X-2, Cyg X-3 (sources in the Cygnus constellation), Her X-1 (a source in the Hercules constellation), etc. However, before the launch of the Uhuru satellite, their nature had remained elusive.

In the 1960s, independently of any observations, several scientists studied theoretical manifestations of black holes and neutron stars. For example, Yakov Borisovich Zel'dovich [4] and Edwin Salpeter [5] drew attention to the energy release in a shock appearing during the supersonic motion of a black hole in a gas cloud (the conic accretion regime).

Theoretical studies of the disc accretion of matter with a high specific angular momentum relative to a gravitating mass [6–8] have been the most successful. Disc accretion naturally emerges in close binary systems consisting of a normal star and a compact star (a neutron star or a black hole). In the course of stellar evolution, the size of the normal star increases, and after it fills its Roche lobe, the transfer of matter from its surface to the region of gravitational attraction of the secondary component begins. In a binary system, due to the orbital relative motion of the components, the matter cannot fall onto the gravitating center but forms a differentially rotating disc-like shell. Due to friction between adjacent layers, the matter strongly heats up and starts glowing. The rapidly rotating disc matter, by gradually losing the angular momentum, slowly moves in the radial direction (accretes) towards the central mass. The glowing of the disc is caused by the gravitational energy release during accretion. The innermost parts of the disc around a black hole are heated up so strongly that they start emitting X-rays. These theoretical developments of disc accretion were carried out almost simultaneously with the Uhuru discovery of accreting black holes and neutron stars in close binary systems.

Measurements of radiation from accretion discs have enabled the discovery of supermassive black holes (with a mass from several million to several billion solar masses) in active galactic nuclei and quasars. The first theoretical results on the emission of discs around supermassive black holes were published by the British astrophysicist Donal Lynden-Bell [9] in 1969. Half a century after that, in April 2019, the results of 1.3 mm observations of the vicinity of the central supermassive black hole in the galaxy M87 were published [10–15]. The observations were carried out using a connected network of eight radio telescopes located in different parts of Earth — the Event Horizon Telescope. These observations enabled for the first time measurements of the sky brightness in the center of the giant elliptical galaxy M87. These observations made it possible to discover a significant decrease in brightness toward the image center, which compellingly proved the existence of a supermassive rotating black hole with a mass of $(6.5 \pm 0.7) \times 10^9 M_\odot$ in the M87 nucleus.

The study of accretion processes is a broad topic in modern high-energy astrophysics. For the advanced reader, we recommend two of our recent monographs *Accretion processes in astrophysics* [16] and *Accretion flows in astrophysics* [17].

This paper is focused on studies of the 35-day (quite nontrivial!) cycle in the X-ray binary Her X-1/HZ Her, whose nature is likely to be related to the complicated behavior of an accretion disc around a freely precessing magnetized neutron star.

2. Properties of X-ray binary system HZ Her/Her X-1

The binary system HZ Her/Her X-1 had been discovered as the X-ray source Her X-1 prior to the launch of the Uhuru satellite, which 'saw' an accreting neutron star in Her X-1 [18]. In the pre-X-ray epoch, the optical star HZ Her was known as an irregular variable star with a high variability amplitude. At that time, nobody could imagine that HZ Her, fact, was a 'regular' variable, the optical component of a close binary system with an accreting neutron star.

After the discovery of the X-ray source, it was recognized that the main reason for the optical variability of HZ Her was heating of the donor star by the X-ray radiation of the neutron star [19, 20] (Fig. 1).

The observed X-ray pulsations with a period of 1.24 s are due to the neutron star's rotation. Their Doppler-modulated times of arrival enabled an orbital period of 1.7 days to be measured. In addition, every 1.7 days the X-ray source is eclipsed for 5.5 hours by the optical donor star during the orbital motion. The presence of the X-ray eclipses suggests a binary orbit inclination close to 90° (i.e., the orbit is seen virtually edge-on).

The X-ray flux modulation with a period of ≈ 35 days is a prominent feature of HZ Her/Her X-1 [21] (see Fig. 2). This 35-day cycle consists of two X-ray 'on'-states with different durations and amplitudes. The first and the second 'on'-states last for ≈ 7 and ≈ 4 orbital periods, respectively. The first 'on'-state (the 'main-on' state) has a higher amplitude than the second (the 'short-on') state. In both cases, the X-ray flux gradually increases to reach a maximum and then smoothly decays. In both 'on'-states, the maximum is shifted towards the turn-on. The X-ray turn-on occurs predominantly near orbital phases 0.2 and 0.7, and the duration of the 35-day cycles is usually 20, 20.5, or 21 orbital periods [22, 23].

The 35-day X-ray modulation can be described by the precession of a warped accretion disc tilted to the orbital plane [24]. The precession is due to the joint action of two torques. The first is caused by tidal forces in the Roche potential. It leads to retrograde (opposite to the orbital motion) precession. The tidal forces are also responsible for the nutation ('swinging') of the disc twice in one orbital period [1] [25, 26]. Due to the tides only, the precession period

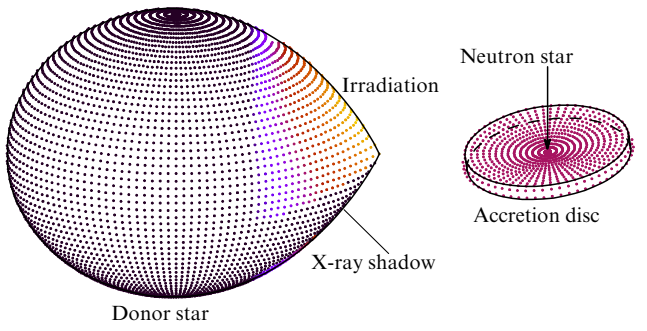

Figure 1. Appearance of the HZ Her/Her X-1.

[1] More precisely, twice the sidereal period $1/P = 1/P_{\rm orb} - 1/P_{35}$, where $P_{\rm orb}$ is the orbital period, and P_{35} is the disc precession period. The minus sign corresponds to retrograde precession.

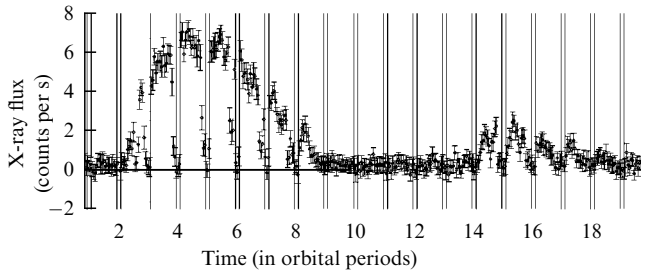

Figure 2. 35-day modulation of the X-ray flux [21].

in the Roche potential would be ≈ 20 days. However, the second torque, which is caused by the dynamical action of gas streams impinging on the disc, acts oppositely to the first one. Thus, the action of the streams slows down the disc precession [27].

The action of the gas streams is variable [27]. In the close binary system HZ Her/Her X-1, the streams are induced by the X-ray heating of the donor star surface near the inner Lagrangian point. If this part of the stellar surface is in the accretion disc 'shadow', the gas flow ceases. Thus, the orbital period the outflow turns off and recommences twice. In one case, the stream impinges on the upper part of the disc; in the other case on the bottom part. Such an intermittent stream action also leads to disc nutation.

The joint action of nutations causes the 'main-on' turn-ons to happen most frequently near two orbital phases,[2] 0.2 and 0.7. Close to these orbital phases, the action of tides and streams adds on, the motion of the disc is somewhat ahead of the mean precessional motion, and the X-ray source opens for the observer with a higher probability.

Multi-year X-ray observations revealed that long-term (up to 1.5 years) 'off'-states of the X-ray source occurred from time to time, but during them the X-ray heating of the donor star did not disappear [28–32]. This means that during these off-states the accretion disc likely lay in the orbital plane and the X-ray source remained obscured to the observer by the disc. It remains unclear which is the physical mechanism forcing the disc to move off the orbital plane and for which reason from time to time the disc lies in the orbital plane.

The archive long-term optical observations of HZ Her fixed by photo plates suggests that there have been long intervals of the absence of X-ray heating irradiation [33, 34]. This means that during these intervals, the accretion onto the neutron star completely ceased.

Let us turn back to the 35-day X-ray modulation. As mentioned above, the flux maximum of the 'main-on' and 'short-on' states is shifted towards the turn-on. At the beginning of the main and short turn-ons, a hard component dominates in the X-ray spectrum. Later on, the spectrum gets softer [35]. Such a spectral behavior can be explained in the model of a twisted disc in which during the precessional motion the inner disc edge is ahead of its outer edge. In this model, the outer cold disc edge opens the X-ray source and the hot inner disc edge with an extended atmosphere eclipses it [36]. In addition, as shown in Section 7, the twisted disc model can also much better explain optical light curves than the flat disc model can.

[2] The orbital phase 0 corresponds to the primary minimum where the neutron star and the disc lie behind the optical star on the line of sight.

The disc can be warped for different reasons: due to a complex dynamical action of gas streams, due to torques caused by outflow (wind) from the disc [37], or due to a magnetic torque from the neutron star applied to the inner disc edge. In our model, we consider the twist caused by the magnetic torque only.

3. Free precession of the neutron star in Her X-1

An analysis of X-ray pulse profiles observed by the RXTE (Rossi X-ray Time Explorer) and Ginga satellites showed them changing periodically with the same 35-day period as the disc precession [38]. The neutron star free precession mechanism was suggested as early as 1972 to explain the 35-day modulation of the observed X-ray flux [39]. The free precession occurs when a body rotates around an axis misaligned with the axes of inertia [40].

Consider a two-axial precession of a neutron star rotating with the angular frequency ω. If the moments of inertia are $I_1 = I_2 \neq I_3$ and the difference between the moments of inertia is small, $|I_3 - I_1| \ll I_1$, the free precession angular velocity reads

$$\Omega = \omega \frac{I_1 - I_3}{I_1} \cos\gamma\,, \tag{1}$$

where γ is the angle between the I_3 inertia axis and the total angular momentum vector, which in this case ($\Omega \ll \omega$) almost coincides with the instantaneous spin axis ω.

From an analysis of the X-ray pulses, in paper [38] the map of emitting regions on the neutron star surface and the angle between the spin axis and the I_3 axis of inertia of the neutron star were recovered. The emitting regions include the north and south magnetic poles surrounded by horseshoe-shaped arcs. The geometry of these regions is due to a complicated nondipole magnetic field near the neutron star surface. In this model, the emitting arcs enclose the I_3 inertial axis, and therefore the storage of accreting matter can produce asymmetry in the principal moments of inertia, $I_3 < I_1 = I_2$. In this case, the sign of the precession frequency in (1) is positive, i.e., the free precession motion coincides with the neutron star rotation. In general, $I_3 \neq I_1 \neq I_2$, and then the neutron star can undergo a more complicated three-axial free precession [41].

The equality of periods of the neutron star free precession and the disc precession is not likely to be coincidental. During the neutron star free precession, the irradiation of the donor star surface changes greatly. The stellar atmosphere heating determines the initial velocity and direction of gas streams flowing through the vicinity of the inner Lagrangian point. In general, the gas streams flow off the orbital plane to form the outer parts of a tilted accretion disc. The dynamic action of the streams affects the disc precession, and therefore, in such a system, the disc precession can occur synchronously with the neutron star free precession. Details of this complicated mechanism are to be clarified by future studies.

4. Magnetic torque acting on the inner parts of the disc

The location of the inner edge of the disc is determined by the break of the disc flow near the magnetospheric boundary at a distance of ~ 100 neutron star radii ($\sim 10^8$ cm). The

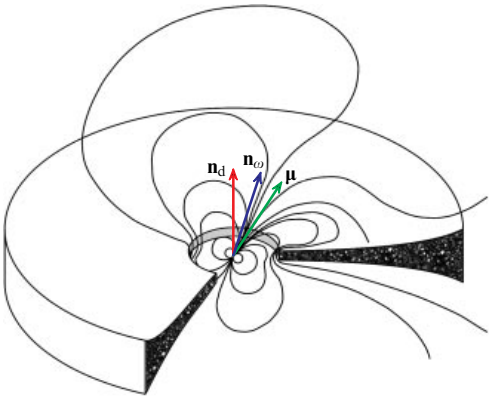

Figure 3. Qualitative structure of the magnetic field around an accreting magnetized neutron star.

magnetic field induces a torque on the inner parts of the disc that, after averaging over the neutron star spin period, takes the form [42–44]

$$\mathbf{K}_m = \frac{4\mu^2}{3\pi R_d^3} \cos\alpha_0 \,(3\cos^2\beta - 1)[\mathbf{n}_\omega, \mathbf{n}_d]\,, \qquad (2)$$

where μ is the neutron star dipole magnetic moment, R_d is the inner disc radius, α_0 is the angle between the neutron star spin and disc axes, β is the neutron star magnetic and spin misalignment angle, and $\mathbf{n}_\omega$ and $\mathbf{n}_d$ are the unit vector along the spin axis and the inner disc rotation, respectively (Fig. 3). The magnetic torque applied to the inner parts of a diamagnetic disc vanishes if $\alpha_0 = 90°$, $\alpha_0 = 0$, and $\beta_0 = \arccos(\sqrt{3}/3) \approx 54.7°$. For $\beta > \beta_0$ and $\beta < \beta_0$, the torque $\mathbf{K}_m$ has different signs.

The magnetic torque forces the inner edge of the accretion disc to lie in the neutron star rotation equator. Then the disc gets warped ('twisted'), with the sign of this characteristic twist being determined by that of the torque $\mathbf{K}_m$. For $K_m = 0$, the twist disappears, and the disc becomes flat.

As shown in [38], the theoretical X-ray profiles best fit the observed ones during the entire precession cycle if the angle between the I_3 axis of inertia and the neutron star spin axis is $\approx 50°$ and the angle between the I_3 axis inertia and the radius-vector to the north magnetic pole is $\approx 30°$ (Fig. 4).

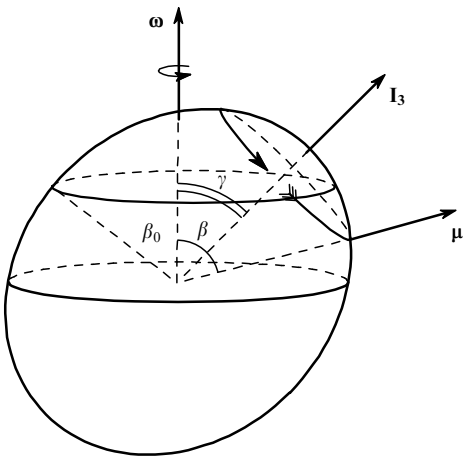

Figure 4. Scheme of the free precession of a neutron star.

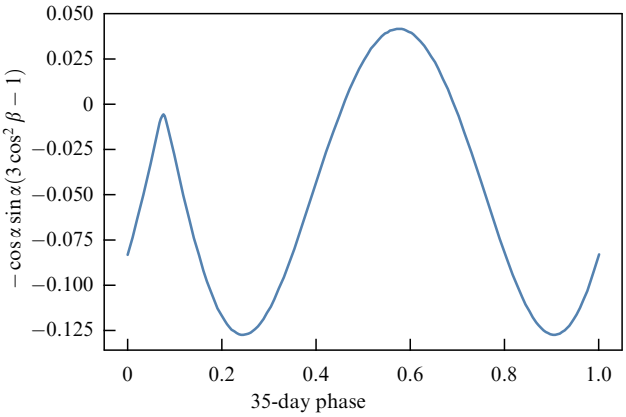

Figure 5. Dimensionless magnetic torque K_m as a function of the 35-day phase. Here, the angles α and β depend on the 35-day phase as $\cos\alpha(x) = \cos\theta\cos\eta_{ns} + \sin\theta\sin\eta_{ns}\cos[2\pi(x + \Delta x_1)]$, where η_{ns} is the angle between the neutron star spin axis and the normal to the orbital plane, θ is the angle between the disc axis and the normal to the orbital plane, $\Delta x_1 = -0.075$; $\cos\beta(x) = \cos\gamma\cos\nu + \sin\gamma\sin\nu\cos[2\pi(x + \Delta x_2)]$, where γ is the angle between the neutron star spin axis and the I_3 inertia axis, ν is the angle between the I_3 inertia axis and the magnetic dipole axis $\boldsymbol{\mu}$, $\Delta x_2 = -0.075$.

In this case, due to neutron star free precession, the angle β changes from $50° - 30° = 20°$ to $50° + 30° = 80°$. Thus, the sign of K_m changes during the precession period twice, and the disc twist should change correspondingly. Furthermore, the angle α_0 in formula (2) should also vary because of the tilted disc precession, and the behavior of the function $K_m(x)$ becomes even more complicated (Fig. 5).

5. B and V optical observations of HZ Her

When constructing optical light curves, we have used the old (1972–1998) B (blue, 5771 points) and V (visual, 5333 points) observations [45–61]. Moreover, in 2010–2019, HZ Her was observed by the authors. Additional 14,034 B-points and 8661 V-points were obtained.

We have used the X-ray turn-ons measured by the Uhuru, Swift RXTE, BATSE (Burst And Transient Experiment), and other X-ray observatories. The time intervals between the consecutive 35-day turn-ons have been divided into 20 equal 0.05-phase segments. Inside each of the segments, an individual light curve has been constructed (Fig. 6). The disc is behind the optical star at the orbital phase 0. A secondary minimum appears at the 35-day phases 0.0–0.35, which is caused by the disc transiting against the heated part of the optical star. At other phases, the secondary minimum is absent because it is projected on the disc shadow on the optical star surface.

At the first four 35-day phases, the light curves close to the end of the orbital phase demonstrate rebrightenings caused by the stream-disc interaction [58, 60, 62]. The origin of these peaks was first studied in paper [63].

6. The model

In this section, we describe the modeling of the optical light curves of HZ Her. The C- and Python codes of the model are available on the web site https://github.com/eliseys/discostar.

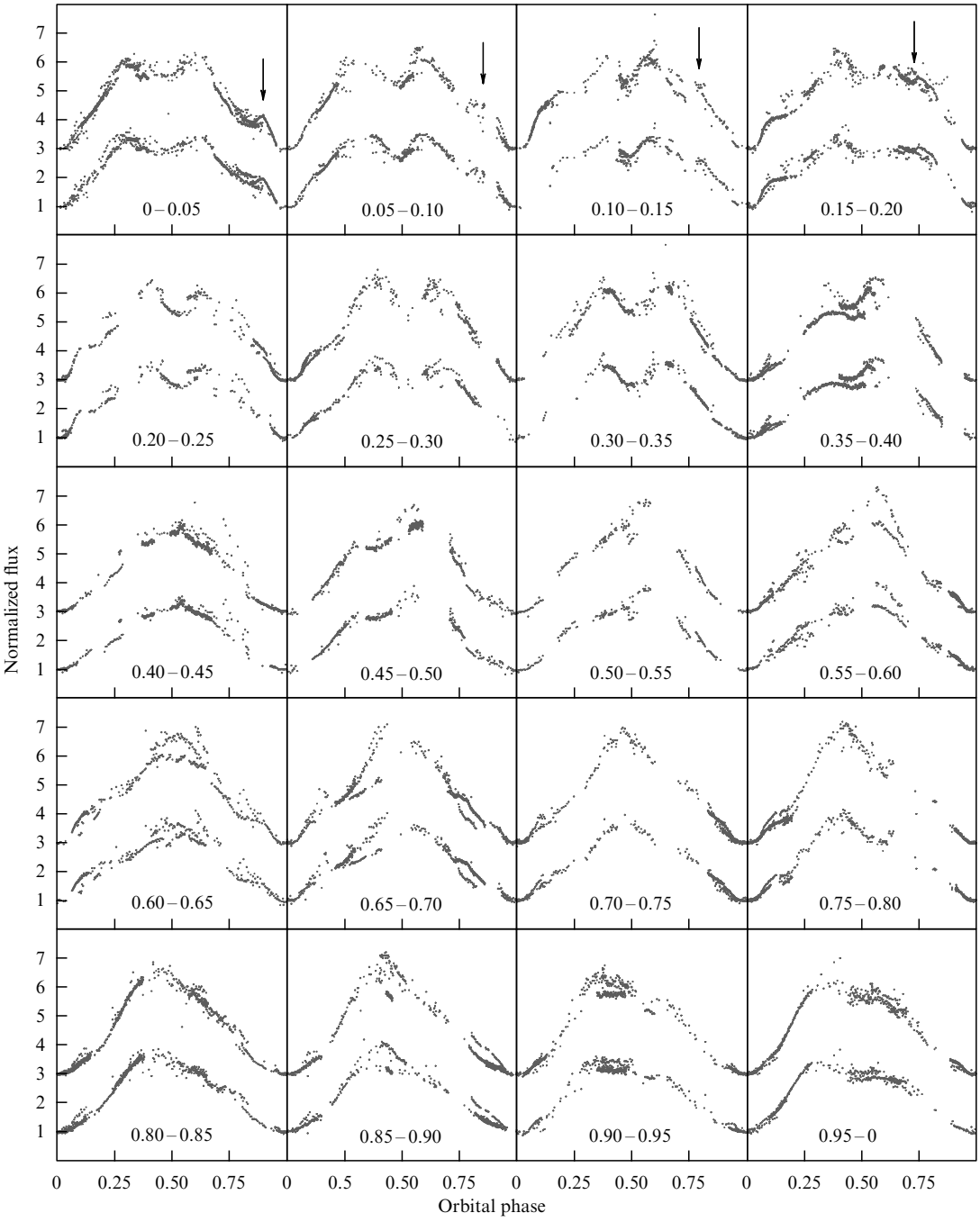

Figure 6. Observed light curves of HZ Her divided into 20 phases of the 35-day cycle. The B-points are shifted upward by two units relative to the V-points. The arrows mark the location of the flux peaks caused by the stream-disc interaction.

6.1 Donor star geometry

The donor star is bounded by the equipotential Roche surface. The dimensionless Roche potential has the form

$$\Omega(q) = \frac{1}{r} + q\left(\frac{1}{\sqrt{1-2x+r^2}} - x\right) + \frac{1}{2}(1+q)(x^2+y^2). \tag{3}$$

Here, $r = \sqrt{x^2+y^2+z^2}$ is the distance from the donor star barycenter. The binary component mass ratio is $q = m_2/m_1$, where m_1 is the donor star mass. The distance between the donor star barycenter and the neutron star is $a = 1$. The value of the potential Ω is chosen such that the equipotential surface touches the inner Lagrangian point L1 corresponding to the inner Roche lobe.

6.2 Donor star surface temperature

The temperature distribution across the donor star surface without X-ray irradiation [3] is determined by the gravitational darkening,

$$T = T_0\left(\frac{g}{g_0}\right)^{\beta}, \tag{4}$$

where $\beta = 0.08$ is for the convective photosphere [64], g is the free-fall acceleration, and g_0 and T_0 are the free-fall accelera-

[3] At the rear of the donor star and in the disc shadow.

tion and temperature at the donor star pole, respectively. The pole temperature is a free parameter, and g is calculated by differentiating equation (3).

In the presence of X-ray illumination, the radiation flux impinging on element $\mathrm{d}\mathbf{S}$ of the donor star surface is

$$\mathrm{d}F_{\mathrm{X}} = I_{\mathrm{X}}(\mathbf{r}_2)\,\frac{\mathrm{d}\mathbf{S}\,\mathbf{r}_2}{r_2}\,, \tag{5}$$

where $\mathbf{r}_2$ is the radius-vector from the neutron star center to the surface element $\mathrm{d}S$. The X-ray intensity is defined by the function $I_{\mathrm{X}}(\mathbf{r}_2)$. The X-ray intensity averaged over the neutron star spin period $\overline{I_{\mathrm{X}}(\mathbf{r}_2)}$ is used to calculate the X-ray heating.

Let A be the fraction of the thermalized X-ray flux; then, in the black-body approximation, the flux from the heated surface element is

$$\sigma_{\mathrm{B}}\,T_{\mathrm{irr}}^4\,\mathrm{d}S = \mathrm{d}F + A\,\mathrm{d}F_{\mathrm{X}} = \sigma_{\mathrm{B}}\,\mathrm{d}S\left(T^4 + A\overline{I_{\mathrm{X}}(\mathbf{r}_2)}\,\frac{\mathrm{d}\mathbf{S}\,\mathbf{r}_2}{r_2}\right). \tag{6}$$

Here, T_{irr} is the effective temperature of the X-ray heated surface element, σ_{B} is the Stefan–Boltzmann constant.

6.3 Accretion disc geometry

In our model, six free parameters fully determine the form and spatial orientation the accretion disc: θ_{out} — the outer disk tilt to the orbital plane, θ_{in} — the inner disc tilt to the orbital plane, φ_{out} — the phase angle of the outer disc precession, Z — the angle between the node line of the outer and inner ring, the binary inclination angle i, and the 35-day phase at which $\varphi_{\mathrm{out}} = 0$. The disc is maximally open to the observer at phase $\varphi_{\mathrm{out}} = 0$. In addition, the semi-thickness of the outer disc edge h that forms the X-ray shadow on the donor star surface is introduced as an additional free parameter.

In our model, the disc is radially split into N rings. The outer ring has the radius $r_0 = R$, while the radii of other rings are much smaller than R:

$$r_k \ll R\,, \quad k = 1, \ldots, N-1\,. \tag{7}$$

Such a disc splitting is chosen because the significant disc warp due to the magnetic torque applied to its inner parts occurs at a distance of ~ 1000 neutron star radii, which is much smaller than the outer disc radius. Beyond ~ 1000 neutron star radii, the disc is considered flat.

The tilt and turn of the k-th ring linearly depend on the number k:

$$\theta_k = \theta_{\mathrm{out}} + k\,\frac{\theta_{\mathrm{in}} - \theta_{\mathrm{out}}}{N-1}\,, \tag{8}$$

$$\varphi_k = \varphi_{\mathrm{out}} + k\,\frac{\varphi_{\mathrm{in}} - \varphi_{\mathrm{out}}}{N-1}\,. \tag{9}$$

The disc form described above is used to calculate the X-ray shadow on the donor star surface. The X-ray flux inside the solid angle between the k-th and $(k+1)$-th rings or inside the solid angle of the outer ring with thickness $2h/R$ is blocked. The donor star parts inside the disc shadow remain unirradiated, and there is no heating effect there.

Near the orbital phase 0.5, the disc passes between the observer and the donor star and screens part of its surface. In this case, ray-tracing technology is used to find the surface elements screened by the disc. These elements do not contribute to the total flux from the binary system. As noted above, the disc is considered flat at radii above ~ 1000 neutron star radii. The model for ray-tracing represents a cylinder of radius R and thickness $2h$. The cylinder inclination θ and its turn φ relative to the orbital plane and the line of sight are equal to the outer disc tilt and turn θ_{out} and φ_{out}, respectively.

6.4 Radiation flux from the disc

In our model, we have not calculated the temperature distribution across the accretion disc, which, taking into account the warp and heating due to the interaction with the gas streams, must be very complicated. The lack of information about the temperature or brightness distribution across the disc surface makes it impossible to correctly model the optical light curve at orbital phases near the eclipse when the disc goes behind the donor star. At these phases, the brightness distribution across the disc is crucial. Therefore, we have modelled the HZ optical light curves only at orbital phases 0.13–0.87 at which the entire disc is open to the observer. Additional fluxes F_{B} and F_{V} in B and V filters are free parameters.

6.5 X-ray radiation intensity

In the model, we have used the calculation of the X-ray emission from a freely precessing neutron star with a complex distribution of the emitting regions across its surface, which provides the best agreement of the theoretical X-ray pulse profiles with observations [38]. The brightest detail on the neutron star surface is the north magnetic pole. The integral X-ray luminosity of the neutron star L_{X} is a free parameter.

As mentioned in Section 4, the free precession occurs around the I_3 inertia axis that makes an angle of $\approx 50^\circ$ with the neutron star spin axis ω. The north magnetic pole is assumed to lie at the north dipole polar cap. The angle between the magnetic dipole $\boldsymbol{\mu}$ and the I_3 axis is $\approx 30^\circ$.

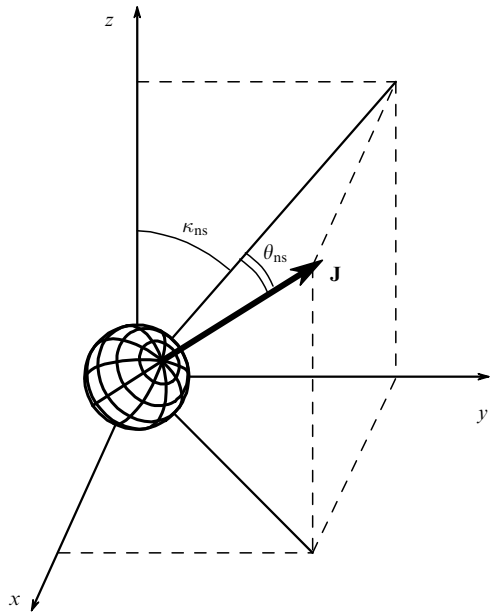

Figure 7. Angles defining the orientation of neutron star angular momentum vector **J** with respect to the observer. The x axis is directed towards the observer, the yz plane is the sky plane. The direction of the z axis coincides with the sky projection of the normal vector to the orbital plane.

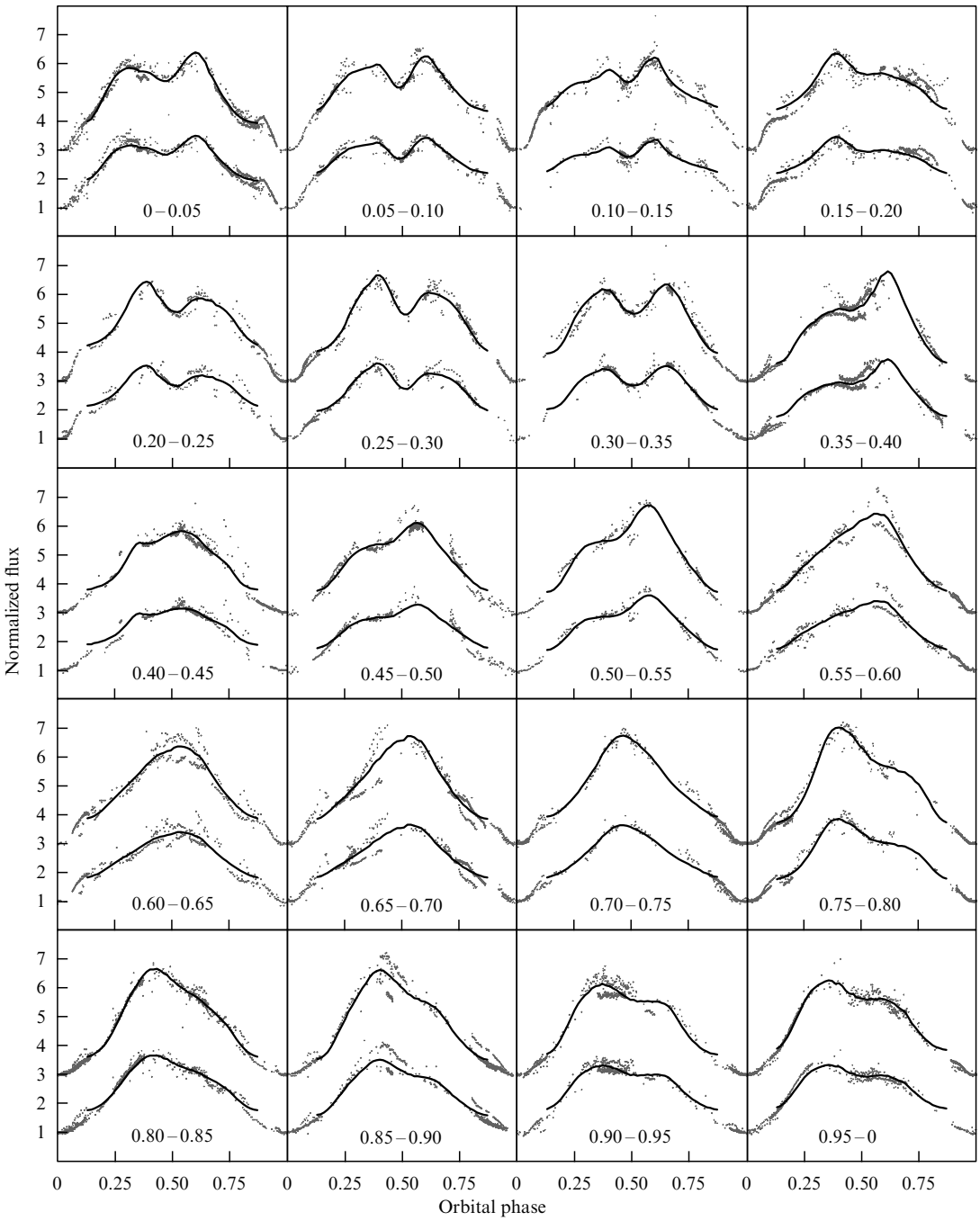

Figure 8. Observed (points) and model (solid lines) B and V light curves. B-points are shifted upwards by two units relative to the V-points. The best-fit light curve is shown at each phase.

The time when the angle between the vector $\boldsymbol{\mu}$ and the neutron star rotational equator is minimal ($\approx 10^\circ$) corresponds to the zero free precession phase Ψ_0. This occurs at the 35-day phase of ≈ 0.05, where the X-ray illumination of the optical star is at the maximum.

According to the model describing X-ray pulse profiles [38], the angle between the neutron star spin axis and the plane perpendicular to the line of sight is $\theta_{\rm ns} = -3^\circ$. The minus sign means that the viewing angle of the neutron star angular momentum vector exceeds 90°. The orientation of the neutron star rotation in the plane perpendicular to the line of sight is a free parameter (Fig. 7).

7. Results of the modeling

The model parameters form two groups. The first one (Table 1) includes parameters which are independent of the 35-day phase. The second group (Table 2) includes parameters which change with the 35-day phase. The aim of the modeling was to find values of parameters minimizing deviations of the model from the observed points for each light curve shown in Fig. 8. The parameters from Table 1 remain fixed during the 35-day cycle, and the parameters from Table 2 are found separately for each light curve.

Table 1. Model parameters fixed at each 35-day phase.

Parameter	Notation	Value	Reference
Major orbital semi-axis	a	6.502×10^{11} cm	[65]
Mass ratio, M_X/M_V	q	0.6448	[65]
Degree of Roche lobe overflow	μ	1.0	
Gravitational darkening coefficient	β	0.08	[64]
Fraction of thermalized X-ray flux*	A	0.5	
Disc radius	R	0.24	[66]
Viewing angle of vector $\mathbf{J}_{ns}$**	κ_{ns}	8.0°	
Viewing angle of vector $\mathbf{J}_{ns}$	θ_{ns}	−3.0°	[38]
Zero phase of neutron star precession	Ψ_0	0.05	[38]
Polar temperature of donor star	T_0	7794.0 K	[65]
Orbital inclination	i	87°	[65]
35-day phase at which $\varphi_{out} = 0$**		0.2	

* Affects L_X only.
** Obtained through item-by-item examination.

Table 2. Model parameters changing with the 35-day phase.

Parameter	Notation	Range
Neutron star X-ray luminosity	L_X	$(0.1-10) \times 10^{37}$ erg s^{-1}
Outer disc tilt	θ_{out}	0–40°
Inner disc tilt	θ_{in}	0–40°
B-flux from disc	F_B	0–4
V-flux from disc	F_V	0–4
Relative thickness of outer disc	h/R	0.05–0.5
Disc phase angle	φ	±20° from linear law
Disk twist	Z	−100°–100° with 10° step

Most of the parameters from Table 1 were fixed using data from the literature (see references in Table 1). Other parameters were found by sorting through possible values. The search for parameters from Table 2 other than the disk twist Z was performed by the Levenberg–Markwardt method. The parameter Z was chosen within the limits from −100° to 100° with a 10° step. Therefore, in Fig. 9, several points corresponding to different Z are shown at each 35-day phase.

In Fig. 8 we present the best-fit B and V model light curves. Generally, good agreement between the model light curves and observed points is seen. Phase 0.15–0.20 is more difficult to model since, at the beginning and at the end of the orbital phase, the observed points are at different levels. The difference is due to disc heating by accretion streams (see the black arrows in Fig. 6). Our model ignores disc irradiation that depends on the orbital phase.

In Fig. 9a, we show the disc phase angle φ_{out} as a function of the 35-day cycle phase. A small deviation, up to ±20°, of the phase angle φ_{out} from the linear law is seen. This is explained by the irregular action of the accretion streams from cycle to cycle, leading to disc nutation over the angle φ.

The color of the circles in Fig. 9 reflects (in correspondence with the color grades on the right-hand side of the figure) the value of the rms deviation s, which is the sum of squares of the deviation of the observed values from the model ones divided by the number of points M at a given phase:

$$s = \frac{1}{M} \sum_{i=1}^{M} \left(y(x_i) - y_i \right)^2 . \qquad (10)$$

Here, y_i, x_i are the flux and orbital phase of an observed point, $y(x)$ is the theoretical light curve. Points with $s > 0.08$ are not shown. At phases 0.60–0.65 and 0.85–0.90, the value of s turns out to be above 0.08, which is related to the large spread of the observed points.

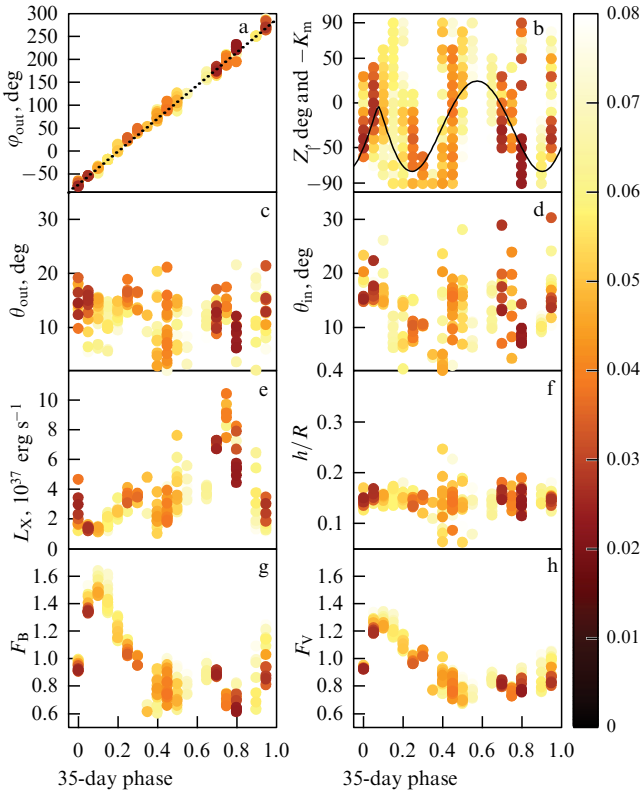

Figure 9. Model parameters as a function of the 35-day phase.

Figure 9c, d show the outer and inner disc tilts θ_{out} and θ_{in} as functions of the 35-day phase. The outer disc tilt slightly

changes around the mean value of 10° – 15°. The outer disc tilt can vary by several degrees due to the joint dynamical action of streams and tides and from cycle to cycle. Thus, the spread of points on the $\theta_{\rm out}$ plot can reflect real changes. The tilt of the inner disc edge is mainly determined by the outer disc inclination and by the magnetic torque applied from the neutron star's magnetic field. At maximum and zero $K_{\rm m}$, the inner disc edge tends to align with the neutron star rotation equator and with the outer disc parts, respectively. It is seen from the figure that at 35-day phases close to 0.2–0.4, 0.6, and 0.8 the inner disc tilt is smaller than the mean outer disk tilt. At these phases, the maximum $K_{\rm m}$ is reached (Fig. 9b).

In Fig. 9b, the disc twist Z and the dimensionless magnetic torque $K_{\rm m}$ are plotted versus the 35-day phase. A significant correlation between the inner disc twist Z and the magnetic torque $K_{\rm m}$ is visible. This suggests that the disc geometry near its inner edge is determined by the interaction with the neutron star magnetosphere.

Figure 9e shows the dependence of the neutron star X-ray luminosity $L_{\rm X}$ on the 35-day phase. The X-ray luminosity increases at phases close to 0.70–0.80. This could be related to the accretion of matter stored in the disc at earlier phases at which the donor illumination was more intensive.

Figures 9g and 9h show B and V fluxes from the disc, respectively, as a function of the 35-day phase. A significant increase in the disc flux is visible, which is related to disc precession and heating.

Figure 9f shows the relative semi-thickness of the outer disc h/R as a function of the 35-day phase. The relative disc semi-thickness does not change significantly: its mean value is around 0.15.

8. Conclusion

The theory of accretion onto compact relativistic objects — neutron stars and black holes in close binary systems — and onto supermassive black holes in galactic nuclei, which was created about half a century ago, is one of the key physical theories that successfully describes multiwavelength observations of these objects. Many details of this theory continue to be studied and developed at the present time. The interested reader can find details and extensive references in our recent monographs [16, 17].

In a present paper, we have considered in more detail accretion processes onto magnetized rotating neutron stars using as a case study the accreting X-ray pulsar Her X-1. The X-ray spectrum of Her X-1 demonstrates a cyclotron resonance scattering feature changing with time (see [67, 68] for more detail and references). This source demonstrates a complex time variability with periods from several seconds (neutron star rotation) to several dozen orbital periods (the accretion disc precession with a period of 35 days) appearing in both the X-ray and the optical ranges. Despite multi-year observations, the nature of the 35-day variability in this source continues to be topical.

We have proposed a possible physical model to explain the 35-day evolution of the X-ray and optical light curves of HZ Her/Her X-1 constructed from multi-year broadband B and V photometrical observations. The key element of the model is a precessing warped accretion disc around a freely precessing neutron star with complex emitting regions around the magnetic poles. The synchronization of the neutron star free precession and the accretion disc precession is due to the interaction of accretion streams with the disc. The intensity of the accretion streams is determined by the X-ray heating of the optical star surface, and the X-ray heating, in turn, is determined by the neutron star free precession phase. Details of the synchronization between the disc precession and the neutron star free precession periods require further research.

Acknowledgements
This study was supported by a grant from the Development Program of Moscow State University, The leading scientific school: the physics of stars, relativistic objects, and galaxies, by RFBR grant 18-502-12025, and DFG grant 259364563.

References

1. Tananbaum H et al. *Astrophys. J.* **165** L37 (1971)
2. Giacconi R et al. *Astrophys. J.* **167** L67 (1971)
3. Giacconi R et al. *Phys. Rev. Lett.* **9** 439 (1962)
4. Zel'dovich Ya B *Sov. Phys. Dokl.* **9** 195 (1964); *Dokl. Akad. Nauk SSSR* **155** 67 (1964)
5. Salpeter E E *Astrophys. J.* **140** 796 (1964)
6. Shakura N I *Sov. Astron.* **16** 756 (1973); *Astron. Zh.* **49** 921 (1972)
7. Shakura N I, Sunyaev R A, in *X- and Gamma-Ray Astronomy, Proc. of Intern. Astronomical Union Symp. No. 55, Madrid, Spain, 11–13 May 1972* (Eds H Bradt, R Giacconi) (Dordrecht: D. Reidel, 1973) p. 155
8. Shakura N I, Sunyaev R A *Astron. Astrophys.* **500** 33 (2009)
9. Lynden-Bell D *Nature* **223** 690 (1969)
10. Akiyama K et al. (Event Horizon Telescope Collab.) *Astrophys. J. Lett.* **875** L1 (2019)
11. Akiyama K et al. (Event Horizon Telescope Collab.) *Astrophys. J. Lett.* **875** L2 (2019)
12. Akiyama K et al. (Event Horizon Telescope Collab.) *Astrophys. J. Lett.* **875** L3 (2019)
13. Akiyama K et al. (Event Horizon Telescope Collab.) *Astrophys. J. Lett.* **875** L4 (2019)
14. Akiyama K et al. (Event Horizon Telescope Collab.) *Astrophys. J. Lett.* **875** L5 (2019)
15. Akiyama K et al. (Event Horizon Telescope Collab.) *Astrophys. J. Lett.* **875** L6 (2019)
16. Abolmasov P K et al. *Akkretsionnye Protsessy v Astrofizike* (Accretion Processes in Astrophysics) (Ed. N I Shakura) (Moscow: Fizmatlit, 2016)
17. Shakura N (Ed.) *Accretion Flows in Astrophysics* (Astrophysics and Space Science Library, Vol. 454) (New York: Springer, 2018)
18. Tananbaum H et al. *Astrophys. J. Lett.* **174** L143 (1972)
19. Cherepashchuk A M et al. *Inform. Bull. Variable Stars* (720) 1 (1972)
20. Kurochkin N E *Peremennye Zvezdy* **18** 425 (1972)
21. Klochkov D K et al. *Astronomy Lett.* **32** 804 (2006); *Pis'ma Astron. Zh.* **32** 593 (2006)
22. Staubert R, Bezler M, Kendziorra E *Astron. Astrophys.* **117** 215 (1983)
23. Shakura N I et al. *Mon. Not. R. Astron. Soc.* **300** 992 (1998)
24. Gerend D, Boynton P E *Astrophys. J.* **209** 562 (1976)
25. Levine A M, Jernigan J G *Astrophys. J.* **262** 294 (1982)
26. Katz J I et al. *Astrophys. J.* **260** 780 (1982)
27. Shakura N I et al. *Astron. Astrophys.* **348** 917 (1999)
28. Parmar A N et al. *Nature* **313** 119 (1985)
29. Vrtilek S D et al. *Astrophys. J. Lett.* **436** L9 (1994)
30. Coburn W et al. *Astrophys. J.* **543** 351 (2000)
31. Boyd P, Still M, Corbet R *The Astronomer's Telegram* (307) 1 (2004)
32. Still M, Boyd P *Astrophys. J.* **606** L135 (2004)
33. Jones C A, Forman W, Liller W *Astrophys. J.* **182** L109 (1973)
34. Hudec R, Wenzel W *Bull. Astron. Inst. Czech.* **27** 325 (1976)
35. Giacconi R et al. *Astrophys. J.* **184** 227 (1973)
36. Boynton P E, in *Physics and Astrophysics of Neutron Stars and Black Holes* (Eds R Giacconi, R Ruffini) (Amsterdam: North-Holland, 1978) p. 111
37. Schandl S, Meyer F *Astron. Astrophys.* **289** 149 (1994)
38. Postnov K et al. *Mon. Not. R. Astron. Soc.* **435** 1147 (2013)
39. Brecher K *Nature* **239** 325 (1972)

40. Landau L D, Lifshitz E M *Mechanics* (Oxford: Pergamon Press, 1976); Translated from Russian: *Mekhanika* (Moscow: Nauka, 1988)
41. Shakura N I, Postnov K A, Prokhorov M E *Astron. Astrophys.* **331** L37 (1998)
42. Lipunov V M, Shakura N I *Sov. Astron. Lett.* **6** 14 (1980); *Pis'ma Astron. Zh.* **6** 28 (1980)
43. Kundt W, Robnik M *Astron. Astrophys.* **91** 305 (1980)
44. Lipunov V M, Semenov E S, Shakura N I *Sov. Astron.* **25** 439 (1981); *Astron. Zh.* **58** 765 (1981)
45. Petro L, Hiltner W A *Astrophys. J. Lett.* **181** L39 (1973)
46. Davidsen A et al. *Astrophys. J. Lett.* **177** L97 (1972)
47. Boynton P E et al. *Astrophys. J.* **186** 617 (1973)
48. Lyutyj V M *Peremennye Zvezdy* **18** 41 (1973)
49. Grandi S A et al. *Astrophys. J.* **190** 365 (1974)
50. Lyutyi V M, Syunyaev R A, Cherepashchuk A M *Sov. Astron.* **17** 1 (1973); *Astron. Zh.* **50** 3 (1973)
51. Cherepashchuk A M et al. *Peremennye Zvezdy* **19** 305 (1974)
52. Voloshina I B, Luytyi V M, Sheffer E K *Sov. Astron. Lett.* **16** 625 (1990); *Astron. Zh.* **16** 625 (1990)
53. Lyutyj V M, Voloshina I B *Pis'ma Astron. Zh.* **15** 806 (1989)
54. Kilyachkov N N, Shevchenko V S *Sov. Astron. Lett.* **4** 191 (1978); *Pis'ma Astron. Zh.* **4** 356 (1978)
55. Kilyachkov N N, Shevchenko V S *Sov. Astron. Lett.* **6** 378 (1980); *Pis'ma Astron. Zh.* **6** 717 (1980)
56. Kilyachkov N N, Shevchenko V S *Sov. Astron. Lett.* **14** 185 (1988); *Pis'ma Astron. Zh.* **14** 438 (1988)
57. Kilyachkov N N et al. *Astron. Lett.* **20** 569 (1994); *Pis'ma Astron. Zh.* **20** 664 (1994)
58. Kippenhahn R, Schmidt H U, Thomas H-C *Astron. Astrophys.* **90** 54 (1980)
59. Gladyshev S A, PhD Thesis. Phys.-Math. Sci. (Moscow: Sternberg Astronomical Institute Moscow Univ., 1985)
60. Mironov A V et al. *Sov. Astron.* **30** 68 (1986); *Astron. Zh.* **63** 113 (1986)
61. Bochkarev N G, Karitskaya E A *Astron Tsirk.* **1433** 1 (1986)
62. Thomas H C et al. *Astron. Astrophys.* **126** 45 (1983)
63. Bochkarev N G, Karitskaya E A, in *Evolutionary Processes in Interacting Binary Stars, Proc. of the 151st. Symp. of the Intern. Astronomical Union, Cordoba, Argentina, August 5–9, 1991* (Eds Y Kondo, R F Sistero, R S Polidan) (Dordrecht: Kluwer Acad. Publ., 1992) p. 449
64. Lucy L B *Z. Astrophys.* **65** 89 (1967)
65. Leahy D A, Abdallah M H *Astrophys. J.* **793** 79 (2014)
66. Paczynski B *Astrophys. J.* **216** 822 (1977)
67. Staubert R et al. *Astron. Astrophys.* **622** A61 (2019)
68. Ji L et al. *Mon. Not. R. Astron. Soc.* **484** 3797 (2019)